

# A Comparison of the Greenshields, Pipes, and Van Aerde Car-Following and Traffic Stream Models

by:

Hesham Rakha<sup>1</sup> and Brent Crowther<sup>2</sup>

## ABSTRACT

The paper compares three car-following models. These models include the Greenshields single-regime model, the Pipes two-regime model, and a four-parameter single-regime model that amalgamates both the Greenshields and Pipes models. The four-parameter model that was proposed by Van Aerde (1995) and Van Aerde and Rakha (1995), is less known but is currently implemented in the INTEGRATION 2.30 software. The Greenshields and Pipes models are considered because they represent state-of-the-practice models for a number of microscopic and macroscopic software. First, the Greenshields model is widely used in macroscopic transportation planning models. In addition, the Pipes model is implemented in a number of microscopic traffic simulation software including the CORSIM and VISSIM software. The paper also relates steady-state car-following behavior to macroscopic traffic stream models in order to develop calibration procedures that can be achieved using macroscopic loop detector data. The study concludes that the additional degree-of-freedom that results from including a fourth parameter (Van Aerde model) overcomes the shortcomings of the current state-of-practice traffic stream models by capturing both macroscopic and microscopic steady-state traffic behavior for a wide range of roadway facilities and traffic conditions. The paper also provides a procedure for calibrating the Pipes car-following model using macroscopic field measurements that can be obtained from loop detectors. This calibration procedure, while it does not overcome the inherent shortcomings of the Pipes model, does provide an opportunity to calibrate the CORSIM and VISSIM car-following behavior to existing roadway conditions more efficiently and without the need to collect microscopic traffic data.

**Key words:** Traffic stream models, car-following models, calibration of microscopic simulation tools, CORSIM, VISSIM, and INTEGRATION.

## 1. INTRODUCTION

Microscopic simulation models use car-following behavior to model the interaction of a vehicle and the preceding vehicle while traveling in the same lane. The process of car-following is modeled as an equation of motion under steady-state conditions plus a number of constraints that govern the behavior of vehicles while moving from one steady-state to another (decelerating and accelerating). Typically up to two constraints are considered. The first constraint governs the vehicle acceleration behavior, which is typically a function of the vehicle dynamics. The second and final constraint ensures that vehicles have a safe position relative to the lead vehicle in order to decelerate to a complete stop without colliding with the preceding vehicle in the event that the preceding vehicle decelerates to a complete stop.

Consequently, the calibration of the car-following behavior within a microscopic simulation model can be viewed as a two-step process. In the first step the steady-state behavior is calibrated followed by a calibration of the non-steady state behavior. The calibration of the steady-state behavior is critical because it dictates the maximum roadway throughput

---

<sup>1</sup> Assistant Professor, Charles Via Department of Civil and Environmental Engineering, Virginia Tech. Virginia Tech Transportation Institute, 3500 Transportation Research Plaza (0536), Blacksburg, VA 24061. E-mail: hrakha@vt.edu

<sup>2</sup> Traffic Engineer, Kimley-Horn & Associates, Suite 250, 7600 North 15<sup>th</sup> Street, Phoenix, AZ 85020. E-mail: Brent.crowther@kimley-horn.com.

(capacity), the speed at which vehicles travel at different levels of congestion (traffic stream behavior), and the spatial extent of queues when fully stopped (jam density). Alternatively, the calibration of the non-steady state behavior, which in most cases is less critical, influences how vehicles move from one steady-state to another and thus captures the capacity reduction that results from traffic break down and the loss of capacity during the first couple of seconds as vehicles depart from a traffic signal (commonly known as the start loss). Under certain circumstances, the non-steady state behavior can influence steady-state behavior. For example, vehicle dynamics may prevent a vehicle from attaining state-state conditions. A typical example of such a case is the motion of a truck along a significant upgrade section. In this case the actual speed of the truck is less than the desired steady-state speed because the vehicle dynamics does not permit the vehicle from attaining its desired speed. The analysis of such instances is beyond the scope of this paper.

## 1.1 Paper Objectives

The objectives of this paper are two-fold. First, the paper presents and compares the Greenshields, Pipes, and Van Aerde car-following models for the modeling of steady-state conditions that occur when the lead and follower vehicles cruise at equal speeds, or the difference in speeds are relatively small that they cannot be perceived by the driver, or the distance headway between the two vehicles is significantly long that the behavior of the lead vehicle has no influence on the behavior of the following vehicle. An analysis of non-steady state conditions, which include moving between steady states that result from differences in vehicle speeds is beyond the scope of this paper and will be presented in a forthcoming paper.

Second, the paper develops an analytical formulation that relates the roadway capacity to the Pipes' model driver sensitivity factor. This important relationship between microscopic and macroscopic traffic behavior provides a unique opportunity to calibrate microscopic car-following models using macroscopic loop detector data. It should be noted, however, that the mechanics of the calibration tool that is required to conduct such a calibration effort is beyond the scope of this paper but will be presented in a forthcoming effort. Instead, the paper compares the various calibrated models to demonstrate differences in car-following behavior without describing how these models were calibrated to field data.

## 1.2 Significance of Research

The significance of this research effort lies in the fact that it not only demonstrates the similarities and differences in the three car-following models, but also explains why differences in model results may occur. The second contribution of this paper is that it provides a procedure for calibrating the Pipes model to macroscopic field data that can be obtained from loop detectors. This calibration procedure would be extremely beneficial for calibrating CORSIM and VISSIM model input parameters to field data. Currently, the calibration of CORSIM is achieved in a rather adhoc manner by changing a driver sensitivity factor until a desired roadway capacity is observed. Specifically, May *et al.* (2001) pointed out that "*direct relationships between desired capacity estimates and CORSIM input parameters were not clear. Research is needed to determine the relationships between the appropriate CORSIM model input parameters and obtaining the desired segment capacity output.*" Alternatively, the literature proposes calibrating the VISSIM car-following behavior by driving a fully-instrumented probe vehicle within the traffic stream to collect car-following data. This approach is extremely expensive and infeasible in most cases.

## 1.3 State-of-the-Art Research

A few studies have attempted to establish the relationship between the Pipes sensitivity factor that is embedded in the CORSIM model and desired capacity estimates. Specifically, Payne *et al.* (1997) performed a series of simulation runs in which the FRESIM model (freeway model within CORSIM) parameters were systematically varied, and the resultant capacity measured. A series of charts were developed from which the car-following sensitivity factor could be obtained by referencing the desired capacity. However, these charts did not account for variations in jam density and free-speed. Furthermore, the relationships were empirically derived, and therefore scenario-specific.

In addition, Halati *et al.* (1997) conducted a series of simulation runs to determine the relationship between the distribution of car-following sensitivity factors and roadway capacity. The study concluded that the mean driver sensitivity factor is a main determinant of roadway capacity. Specifically, the study concluded that the mean value of the decile distribution of sensitivity factors was important, and that the variance appeared to have a lesser impact on the roadway capacity. Halati *et al.* finding is critical to the procedures that are developed in this paper because the proposed analytical procedures estimate the average driver sensitivity factor that is to be input to the simulation model in order to obtain a desired roadway capacity.

## 1.4 Paper Layout

The paper first provides a brief background of car-following models that describe the behavior of vehicles as they follow a lead vehicle. Having described the behavior of a pair of vehicles, the behavior of a traffic stream of vehicles is described. Specifically, a number of standard macroscopic functional relationships are described including single- and multiple-regime models. The relationship between car-following and macroscopic traffic flow behavior is then introduced. Subsequently, three steady-state car-following models are presented. The paper then develops analytical relationships that allow the user to calibrate these three car-following models using readily available loop detector data. Finally, the conclusions of the paper are presented.

## 2. BACKGROUND

This section describes a number of standard single- and multi-regime macroscopic traffic stream models that have been described in the literature. These macroscopic models identify the relationship between the three traffic flow parameters, namely flow, speed, and density. While macroscopic traffic flow models describe the behavior of a stream of vehicles along a roadway stretch, microscopic car-following models describe the behavior of a pair of vehicles within a traffic stream. The importance of relating steady-state car-following behavior to macroscopic traffic flow parameters stems from the fact that, unlike microscopic behavior, macroscopic traffic flow parameters can be measured fairly easily in the field using standard loop detectors or traffic counters. Consequently, the calibration of the car-following models is more easily achieved using macroscopic parameters as will be described later in the paper.

### 2.1 Microscopic Steady-State Car-Following Models

Initially the car-following behavior of a single vehicle is explained prior to describing how the motion of a single vehicle affects the flow of an entire traffic stream. It should be noted at this point that this section only describes car-following behavior under steady-state conditions, when the lead vehicle is traveling at a constant speed and both the lead and follower vehicles have an identical car-following behavior. Steady-state car-following is extremely critical given that it influences the overall behavior of the traffic stream. Specifically, steady-state behavior determines the desirable speed of vehicles at different levels of congestion, the roadway capacity, and the spatial extents of queues. Clearly, these factors have significant impacts on the formation of queues and extent to which queues spillback onto upstream roadways.

#### 2.1.2 Field Data

Under steady-state conditions given that the speed differential between the lead and following vehicle approaches zero, current state-of-practice car-following behavior resolves to a relationship between the vehicle speed and its distance headway from the lead vehicle. The relationship tends to an asymptotic maximum speed (termed the free-speed) as the headway approaches infinity, as illustrated in Figure 1. In other words, at free-speed the vehicle's desired speed is not governed by the surrounding traffic; instead it is governed by roadway friction, regulatory, and/or roadway geometric conditions. As the distance headway between the subject and lead vehicle decreases the desired vehicle speed decreases until the vehicle comes to a complete stop. It should be noted from Figure 1 that field data tend to demonstrate a fairly linear increase in speed as a function of the distance headway for freeway facilities where the vehicle is less constrained by the roadway geometry and/or friction but is more constrained by regulatory conditions

(e.g. speed limit). Alternatively, data that were obtained from the Holland Tunnel in New York demonstrate a non-linear car-following behavior. The Holland Tunnel is a two-lane directional roadway underneath the Hudson River that connects New Jersey to New York. The design features of the tunnel are somewhat restrictive, with 3.3-meter lanes (11-foot lanes), no shoulders, and a typical tunnel alignment consisting of a downgrade followed by an upgrade. These data that were recorded by the Port of New York Authority as part of their surveillance system were aggregated into 5-minute averages (May, 1990). The car-following model that is calibrated to the data demonstrates a less aggressive driving behavior compared to freeway driving as demonstrated by the milder slope in the speed-headway relationship.

Finally, the arterial data that were obtained from a Newcastle University research team in the United Kingdom who were studying incident detection technologies (May, 1990), demonstrate an even less aggressive driving behavior with a significant non-linear car-following model. Unlike the freeway and tunnel-driving environment, the arterial roadway constitutes driving in an environment that is classified as uncontrolled with vehicles encountering significant roadway friction.

It should be noted that the field data that are presented in Figure 1 were extracted from a number of data sources, as was described earlier. These data represent driving conditions in a number of controlled and uncontrolled environments. The car-following models that are calibrated to the field data, which will be described later in the paper, represent the steady-state car-following behavior of a vehicle. As was mentioned earlier, vehicles will typically move from one steady state to another along this car-following relationship. The vehicle's ability to move between steady states is constrained by its acceleration and deceleration capabilities, by the driver aggressiveness, and by weather and pavement conditions.

### 2.1.2 State-of-the-Art Car-Following Models

Theories describing how vehicles follow one another were developed in the 1950s and 1960s (May, 1990) and continue to be developed and compared (Aycin and Benekohal, 1999). As was mentioned earlier, the majority of car-following models consider two independent variables in the driver's speed selection decision. These variables include the distance headway and the speed differential between the lead and follower vehicle. The models make a simplifying assumption that drivers only respond to the vehicle ahead of them without observing other vehicles further downstream. In some instances the models consider a driver reaction time with its traffic stability repercussions.

In order to fulfill the objectives of the paper, three car-following models are presented. These models include the Pipes model because it serves as the basis for a number of microscopic simulation models including the CORSIM and VISSIM steady-state car-following logic, the car-following model that evolves from the Greenshields macroscopic traffic stream model, and a four-parameter model (Van Aerde model) that combines both the Pipes and Greenshields models. The Van Aerde model constitutes the steady-state car-following logic within the INTEGRATION 2.30 software.

Pipes characterized the motion of vehicles in a traffic stream as following a linear relationship, as illustrated in Figure 2. The car-following behavior of a vehicle is constrained by a maximum speed, which is commonly known as the free-speed. Free-flow speed or free-speed is the desired travel speed of a vehicle when the distance headway tends to infinity (i.e. no other vehicles are on the roadway). The free-speed is typically slightly higher than the speed limit of the roadway and depends on the level of highway surveillance. The slope of the Pipes model has been calibrated to reflect the data for the various facilities that are presented in the figure.

Figure 2 further illustrates the car-following behavior that results from the Greenshields macroscopic traffic stream model that is described in the forthcoming section and the Van Aerde model that is also illustrated in Figure 1. Figure 2 clearly illustrates that the Pipes model structure (linear car-following model) does not capture field observed car-following behavior over a wide range of facility types and car-following domain.

## 2.2 Macroscopic Traffic Stream Models

Having characterized the motion of a pair of vehicles, this section describes the behavior of an entire traffic stream that evolves from the car-following logic of the individual vehicles that constitute this traffic stream. Traffic stream models

provide the fundamental relationships between three macroscopic traffic stream parameters for steady-state conditions, as illustrated in Figure 3. The traffic stream parameters include flow, speed, and density. A unique flow parameter is the maximum flow or capacity ( $q_c$ ), which corresponds to the x-coordinate at the nose of the speed-flow relationship. Two unique parameters are identified on the speed-flow relationship, which include the free-speed ( $u_f$ ) and speed-at-capacity ( $u_c$ ). The speed-at-capacity is the speed that exists at maximum flow conditions and corresponds to the y-coordinate of the nose of the speed-flow relationship, as illustrated in Figure 3. The two unique density parameters include jam density ( $k_j$ ) and density-at-capacity ( $k_c$ ), often referred to as the optimum density. Jam density is the density of traffic when both flow and speed approach zero. The basic traffic stream model establishes flow as the product of density and speed, as demonstrated in Equation 1.

$$q = ku \quad [1]$$

### 2.2.1 Field Data

In order to demonstrate how traffic stream models vary for different facility types, the three different data sets that were presented earlier are presented again in the speed-flow-density domain. Specifically, Figure 3 illustrates the I-4 freeway data from Orlando, Florida, while Figure 4 illustrates the data from the Holland Tunnel in New York, and Figure 5 illustrates the loop detector data that were collected on an arterial roadway in the United Kingdom. Superimposed on the figures are calibrated speed-flow-density relationships that were generated using a calibration based on the Van Aerde model structure with a calibration tool that will be described in a forthcoming publication.

The freeway speed-flow relationship demonstrates a fairly constant speed in the uncongested regime of the relationship (speeds in excess of speed-at-capacity), as illustrated in Figure 3. This trend is caused by the fact that the vehicles traveling under uncongested conditions are not constrained by vehicle-to-vehicle interaction; instead vehicles are constrained by the speed limit of the facility (90 km/h). The figure also demonstrates that the speed-density relationship is highly non-linear exhibiting an S-shaped relationship. The flow-density relationship exhibits a low level of variability about the calibrated model in the uncongested regime (densities less than the density-at-capacity) with more variability in the congested regime.

The tunnel data exhibit a more parabolic type of speed-flow relationship with a more linear trend in the speed-density domain, as illustrated in Figure 4. Comparing Figure 3 to Figure 4 it is evident that the vehicles are more constrained with the vehicle interactions in the case of the tunnel than in the case of the freeway facility. The figures also demonstrate a higher lane capacity in the range of 2000 veh/h on the freeway versus a 1300 veh/h capacity along the tunnel facility. The capacity of the arterial roadway is further reduced to 600 veh/h as a result of various forms of friction along the facility and the impact of traffic signal timings on the facility capacity.

### 2.2.2 State-of-the-Art Traffic Stream Models

Over the years a number of traffic stream models have been proposed and described in the literature. The earlier models assumed a single regime for the congested and uncongested conditions. Later models attempted to improve on the single-regime models by introducing separate models for the uncongested and congested regimes.

The most famous of the single regime models is Greenshields' model that was developed in 1934 based on observations of speed-density measurements obtained from an aerial photographic study (May, 1990). Using these data Greenshields concluded that speed was a linear function of density, as demonstrated in Equation 2. Using the linear speed-density relationship together with the basic traffic stream model that was presented in Equation 1, the speed-flow relationship is represented as a parabolic relationship, as demonstrated in Equation 3. The speed-at-capacity can be computed by taking the derivative of the flow with respect to speed, as demonstrated in Equation 4. This relationship results in a speed-at-capacity that is equal to half the free-speed. The traffic stream relationships that correspond to the Greenshields model are illustrated in Figure 6. It is clear by comparing Figure 6 to the field data that are presented in Figure 3, Figure 4, and Figure 5 that the parabolic speed-flow relationship is reflective of field data under limited conditions. Finally, it should be noted that the calibration of the Greenshields' model requires the estimation of two parameters, namely the free-speed and either the jam density or the capacity.

$$u = u_f - \frac{u_f}{k_j} k \quad [2]$$

$$q = \frac{k_j}{u_f} (u_f - u)u = k_j \left( u - \frac{u^2}{u_f} \right) \quad [3]$$

$$\left. \frac{\partial q}{\partial u} \right|_{u_c} = 1 - \frac{2u_c}{u_f} = 0 \quad [4]$$

### 2.3 Relationship Between Macroscopic Traffic Stream and Steady-State Car-Following Behavior

As was mentioned earlier given that steady-state microscopic car-following models characterize the relationship between the vehicle's desired speed and the distance headway between the lead and follower vehicles, this model can be related to the macroscopic speed-density relationship assuming all vehicles in the traffic stream maintain the same headway distance or have an average headway distance that is consistent with the car-following model.

For example, Drew (1968) indicates, "*the similarities in the macroscopic and microscopic approaches have been emphasized. The former solves a differential equation of stream motion and a differential equation of continuity, both expressed in terms of speed 'u' and density 'k' to obtain an equation of state (the equation of the fundamental q-u-k traffic surface). The latter combines the differential equation of motion for an individual vehicle together with the appropriate boundary conditions to obtain an equation of state.*"

### 3. GREENSHIELDS' CAR-FOLLOWING MODEL

Because the four-parameter or Van Aerde model that is described later provides more degrees of freedom to capture the range of behavior across different regimes and facility types; as illustrated in Figure 3, Figure 4, and Figure 5; comparisons are made against the more general Van Aerde model.

The car-following model that corresponds to the Greenshields' traffic stream model is derived from Equation 2, as demonstrated in Equations 5, 6, and 7. The corresponding car-following behavior that evolves from the Greenshields' model demonstrates a fairly aggressive car-following behavior at short distance headways with a less aggressive car-following behavior at longer headways, as demonstrated in Figure 2.

$$k = \frac{k_j}{u_f} (u_f - u) = \frac{(u_f - u)}{k_j / u_f} \quad [5]$$

$$\frac{1}{h} = \frac{(u_f - u)}{k_j / u_f} \quad [6]$$

$$h = \frac{c_2}{(u_f - u)} \quad [7]$$

A comparison of the Greenshields and Van Aerde models for the I-4 freeway data, as illustrated in Figure 6, demonstrates that the Greenshields parabolic speed-flow relationship and its corresponding linear speed-density relationship are inconsistent with the field data. Specifically, the data indicate that vehicles travel at a speed that is higher than half the free-speed when traveling at capacity.

It should be noted at this point that the calibrated jam density for the Greenshields model is different from the calibrated jam density for the Pipes and Van Aerde models because the Greenshields model requires the calibration of two

parameters; the free-speed and capacity. Once these two parameters are calibrated the jam density can be computed as twice the density at capacity, which is based on the roadway capacity and free-speed ( $4q_j/u_f$ ).

The Holland Tunnel data that were illustrated in Figure 4 indicate a more parabolic speed-flow relationship, as illustrated in Figure 7. However, the speed-density domain clearly indicates that a linear speed-density relationship does not reflect the data. The Holland Tunnel data demonstrate a very important concept, namely that a good fit in one domain (e.g. speed-flow) does not necessarily imply a good fit in another domain (e.g. speed-density). Similarly, data collected along an arterial street, as illustrated in Figure 5 indicate a parabolic behavior in the speed-flow domain with a non-linear speed-density relationship, as illustrated in Figure 8.

The three facility types that are illustrated in Figure 6, Figure 7, and Figure 8 clearly demonstrate the deficiency of the Greenshields' model in capturing the steady-state behavior of a wide variety of facility types for the full range of traffic flow data domains.

## 4. PIPES CAR-FOLLOWING MODEL

As was mentioned earlier the Pipes model constitutes the steady-state car-following model in a number of microscopic simulation software, including CORSIM and VISSIM. This section briefly describes the car-following models that are incorporated in the CORSIM and VISSIM software and demonstrates that under steady-state conditions these models revert to the Pipes car-following model. This section provides a very brief overview of the car-following logic within the CORSIM and VISSIM models. More detailed information can be obtained from the literature.

The traffic stream models that evolve from the Pipes car-following model are multi-regime in the sense that a different model is utilized for the congested versus uncongested regimes, as illustrated in Figure 6. Specifically, the Pipes model assumes that the traffic stream speed is insensitive to the traffic density in the uncongested regime. This assumption best fits roadways that are designed under high geometric standards when vehicle speeds are constrained by regulatory constraints rather than the surrounding traffic (e.g. speed limit), however, the assumption is less valid for roadways with sub-standard geometric designs or with significant roadway friction, as demonstrated in Figure 6, Figure 7, and Figure 8.

### 4.1 CORSIM Car-Following Behavior

CORridor SIMulation (CORSIM) is the micro-simulation component of the TRAF family of models that were developed by the US Federal Highway Administration (FHWA) for simulation of traffic behavior on integrated urban transportation networks of freeway and surface streets. CORSIM combines the NETwork SIMulation (NETSIM) and FREeway SIMulation (FRESIM) models into an integrated package. Both NETSIM and FRESIM simulate traffic behavior at a microscopic level with detailed representation of individual vehicles and their interaction with their physical environment and other vehicles.

#### 4.1.1 FRESIM Car-Following Behavior

The FRESIM model utilizes the Pitt car-following behavior that was developed by the University of Pittsburgh (Halati *et al.*, 1996). The basic model incorporates the distance headway and speed differential between the lead and follower vehicle as two independent variables, as demonstrated in Equation 8. As was mentioned earlier, given that steady-state conditions are characterized by travel at an equal constant speed by both the lead and follower vehicles, the third term of the car-following model tends to zero under steady state driving. Consequently, the steady-state car-following model that is incorporated within FRESIM can be characterized by Equation 9 in the congested regime and a constraint of maximum speed on the roadway, as demonstrated in Equation 10 (uncongested regime). This car-following behavior is identical to the Pipes model that was described earlier.

$$h = h_j + c_3 u + bc_3 \Delta u^2 \quad [8]$$

$$h = h_j + c_3 u \quad [9]$$

$$u = \min\left(\frac{h - h_j}{c_3}, u_f\right) \quad [10]$$

Where:

$h$  = distance headway between front bumper of lead vehicle and front bumper of follower vehicle (km),

$h_j$  = distance headway when vehicles are completely stopped in a queue (km),

$c_3$  = driver sensitivity factor (h),

$b$  = calibration constant that equals 0.1 if the speed of the follower vehicle exceeds the speed of the lead vehicle, otherwise it is set to zero,

$\Delta u$  = difference in speed between lead and follower vehicle, and

$u_f$  = roadway free-speed.

#### 4.1.2 NETSIM Car-Following Behavior

The basic car-following model within NETSIM is defined in Equation 11. Using the conditions of steady-state travel Equation 11 can be simplified to Equation 12. This simplification results from the fact that the stopping distance for both the lead and follower vehicles are identical given their equal speeds. In addition, no driver reaction is required because the follower and lead vehicles are traveling at constant speeds (steady-state flow). Furthermore, given that the distance traveled during a time increment  $\Delta t$  is the product of the vehicle speed and the time duration ( $\Delta t$ ) and because NETSIM utilizes a time step of 1 second, the steady-state car-following model reverts to the Pipes model with a driver sensitivity factor of 1.0 (assuming speed is in ft/s and distance is in ft), as demonstrated in Equation 13.

$$h = h_j + \Delta s + \Delta r + S_F - S_L \quad [11]$$

$$h = h_j + u\Delta t \quad [12]$$

$$h = h_j + u \quad [13]$$

Where:

$\Delta s$  = distance traveled by follower vehicle over time interval  $\Delta t$  (km)

$\Delta r$  = distance traveled by follower vehicle during its reaction time (km)

$S_F$  = distance required by follower vehicle to come to a complete stop (km)

$S_L$  = distance required by lead vehicle to come to a complete stop (km)

#### 4.2 VISSIM Car-Following Model

The VISSIM model uses a psycho-physical car-following model (Fellendorf and Vortisch, 2000). The model incorporates the Pipes car-following logic at its core, as defined in Equation 10. The model also considers other factors that include; randomness in the jam density headway, the speed difference between lead and follower vehicles, the distance headway that the vehicle reacts to a speed difference, and the driver's perception of the speed difference. Consequently, as is the case for the CORSIM model, under steady-state conditions the car-following logic within VISSIM reverts to the Pipes model.

#### 4.3 Proposed Procedures for Calibrating the Pipes Car-Following Model

The Pipes model represents a linear increase in the travel speed as the distance headway increases. The driver sensitivity factor ( $c_3$ ) defines the slope of the speed-headway relationship, while the intercept with the x-axis defines the jam density headway ( $h_j$ ) of traffic, as illustrated in Figure 2. A third parameter that is required in characterizing the speed-headway relationship is the free-speed, or the maximum speed of travel when a vehicle is not constrained by the surrounding traffic. Consequently, the Pipes car-following model requires the calibration of three parameters, namely; the free-speed, the jam density headway, and the driver sensitivity factor. While free-speed is relatively easy to estimate

in the field and generally lies between the speed limit and the design speed of the roadway, jam density headway is more difficult to calibrate but typically ranges between 110 to 150 vehicles/km/lane. The driver sensitivity factor is extremely difficult to calibrate because it is not measured using standard surveillance technologies (e.g. loop detectors).

Two common procedures have been utilized to calibrate the Pipes model within the CORSIM and VISSIM software. The first procedure involves a trial-and-error approach that entails changing the driver sensitivity factor until a desired roadway capacity is observed. This approach, however, is network specific and time consuming. The alternative procedure, which has been applied to VISSIM, involves driving an instrumented probe vehicle along the roadway to collect data. This approach, however suffers from a number of shortcomings. First, it is extremely expensive to instrument a vehicle for purposes of data collection deeming it unrealistic. Second, the approach is driver dependent., which would require extensive data collection in order to include different driver behaviors. Third, it is difficult to collect data along the entire range of the speed-headway relationship. Forth, differences in the speed-headway behavior will occur depending on the facility type, as was clearly demonstrated earlier in the paper. Consequently, this paper proposes a calibration procedure that can be applied using readily available loop detector data.

The derivation of the proposed functional form involves two steps. The first step is to demonstrate that the functional form of the Pipes model is a strict monotonic function. Second, having demonstrated that the function is strictly monotonic the driver sensitivity factor can be related to the roadway capacity, which can be estimated from loop detector data.

The Pipes car-following relationship in the congested regime is characterized by Equation 14. Since traffic stream density is the inverse of the space headway, Equation 15 describes the basic speed-density relationship that evolves from the Pipes car-following model.

$$h = h_j + c_3 u \quad [14]$$

$$k = \frac{1}{h_j + c_3 u} \quad [15]$$

Using the basic traffic stream relationship that is defined in Equation 1 in conjunction with Equation 15 the speed-flow relationship can be derived, as demonstrated in Equation 16.

$$q = \frac{u}{h_j + c_3 u} \quad [16]$$

The slope of the speed flow relationship is computed as the derivative of flow with respect to speed as demonstrated in Equation 17. The final form of the slope that as computed by Equation 18 is a strict monotonic function given that the jam density headway of vehicles is non-negative and non-zero. Consequently, the maximum flow will occur at the extreme point (i.e. at the maximum speed which is the free-speed).

$$\frac{\partial q}{\partial u} = \frac{\partial}{\partial u} \left( \frac{u}{h_j + c_3 u} \right) = \frac{1}{h_j + c_3 u} - \frac{c_3 u}{(h_j + c_3 u)^2} \quad [17]$$

$$\frac{\partial q}{\partial u} = \frac{h_j}{(h_j + c_3 u)^2} \quad \text{Where : } h_j > 0 \quad [18]$$

Using Equation 16 and recognizing the fact that the speed-flow relationship is strictly monotonic, the maximum flow ( $q_c$ ) occurs at the boundary of the relationship (i.e. at free-speed). Consequently, the maximum flow can be derived from Equation 16 by substituting the flow for the capacity of the roadway ( $q_c$ ) and the speed for the free-speed ( $u_f$ ). Using Equation 19, the driver sensitivity coefficient can be computed, as defined in Equation 20. Equation 20 requires three parameters that can be obtained from standard loop detector data. These parameters include the roadway capacity (maximum flow rate), the spacing of vehicles at jam density, and the roadway free-speed.

$$q_c = \frac{u_f}{h_j + c_3 u_f} \quad [19]$$

$$c_3 = \frac{1}{q_c} - \frac{h_j}{u_f} \quad [20]$$

## 5. VAN AERDE CAR-FOLLOWING MODEL

The INTEGRATION model (M. Van Aerde and Associates, 2001a and 2001b) uses a steady-state car-following model that was proposed by Van Aerde (1995) and Van Aerde and Rakha (1995), which combines the Pipes and Greenshields models into a single-regime model. The model, which requires four input parameters, can be calibrated using field loop detector data. The details of the calibrating procedure are beyond the scope of this paper but will be described in detail in a forthcoming publication.

The functional form of the Van Aerde model amalgamates the Greenshields and Pipes car-following models, as demonstrated in Equation 21. This combination provides the functional form with an additional degree of freedom by allowing the speed-at-capacity to be different from the free-speed. Specifically, the first two parameters provide the linear increase in the vehicle speed as a function of the distance headway, while the third parameter introduces curvature to the model and ensures that the vehicle speed does not exceed the free-speed. The addition of the third term allows the model to operate with a speed-at-capacity that does not necessarily equal the free-speed, as is the case with the Pipes model.

In summary, the Van Aerde single-regime model combines the Greenshields and Pipes models in order to address the main flaws of these models. Specifically, the model overcomes the shortcoming of the Pipes model in which it assumes that vehicle speeds are insensitive to traffic density in the uncongested regime, which has been demonstrated to be inconsistent with a variety of field data from different facility types, as illustrated in Figure 3, Figure 4, and Figure 5. Alternatively, the model overcomes the main shortcoming of the Greenshields model, which assumes that the speed-flow relationship is parabolic, which again is inconsistent with field data from a variety of facility types, as demonstrated in Figure 3, Figure 4, and Figure 5.

It is sufficient to note at this time that the calibration of the car-following model requires estimating four parameters, namely  $c_1$ ,  $c_2$ ,  $c_3$  and  $k$  utilizing Equations 22a, 22b, 22c, and 22d. These four parameters are a function of the roadway free-speed, the speed-at-capacity, capacity, and jam density. The derivation of these four equations is presented in Appendix C using a number of boundary conditions including the maximum flow and jam density boundary conditions.

$$h = c_1 + c_3 u + \frac{c_2}{u_f - u} \quad [21]$$

$$m = \frac{2u_c - u_f}{(u_f - u_c)^2} \quad [22a]$$

$$c_2 = \frac{1}{k_j \left( m + \frac{1}{u_f} \right)} \quad [22b]$$

$$c_1 = m c_2 \quad [22c]$$

$$c_3 = \frac{-c_1 + \frac{u_c}{q_c} - \frac{c_2}{u_f - u_c}}{u_c} \quad [22d]$$

Where:

$c_1$  = fixed distance headway constant (km),

$c_2$  = first variable distance headway constant ( $\text{km}^2/\text{h}$ ),

$c_3$  = second variable distance headway constant (h),

$u_f$  = free-speed (km/h),

$u_c$  = speed at capacity (km/h),

$q_c$  = flow at capacity (veh/h),

$k_j$  = jam density (veh/km), and

$m$  = is a constant used to solve for the three headway constants (h/km).

## 6. FINDINGS AND CONCLUSIONS

Three macroscopic traffic stream models and their corresponding microscopic steady-state car-following models were presented in this paper. The simplest of these models, namely the Greenshields' single-regime model requires two calibrated parameters: free-speed and either capacity or jam density. Alternatively, the Pipes' two-regime car-following model requires three calibrated parameters: free-speed, jam density, and a driver sensitivity factor. Finally, the four-parameter single-regime model that was proposed by Van Aerde (1995) and Van Aerde and Rakha (1995), while requiring four parameters for calibration, provides more degrees of freedom to reflect different traffic behavior across different roadway facilities. Specifically, Figure 3, Figure 4, and Figure 5 demonstrate the ability of the Van Aerde model to reflect traffic stream behavior from a number of varying facility types including a freeway, an arterial, and a tunnel roadway. These fits demonstrate a good representation of the steady-state macroscopic behavior of a traffic stream in the flow, speed, and density domains. Furthermore, Figure 1 illustrates a good representation of steady-state car-following behavior for the three facility types that were considered.

The additional degree-of-freedom that is provided by including four parameters in the microscopic car-following and macroscopic traffic stream models overcomes the shortcomings of the current state-of-practice models by capturing both macroscopic and microscopic steady-state traffic behavior for a wide range of roadway facilities. Specifically, Figure 6, Figure 7, and Figure 8 clearly demonstrate the shortcomings of both the Greenshields and Pipes models in capturing the full range of traffic stream behavior for a single facility in addition to capturing differences in traffic behavior over different facilities.

Finally, the proposed modification to the calibration procedures of the Pipes model offers an avenue to calibrate microscopic car-following behavior using macroscopic field measurements that are readily available from loop detectors. This calibration procedure, while it does not overcome the inherent shortcomings of the Pipes model, does provide an opportunity to better calibrate the CORSIM and VISSIM car-following behavior to existing roadway conditions.

## REFERENCES

- Aycin M.F. and Benekohal R.F. (1999), *Comparison of Car-Following Models for Simulation*, Transportation Research Record, No. 1678, pp. 116-127.
- Drew D. (1968), *Traffic Flow Theory and Control*, McGraw Hill.
- Halati A., Lieu H., and Walker S. (1997) "CORSIM- Corridor Traffic Simulation Model," Proceedings ASCE Conference on Traffic Congestion and Safety in the 21<sup>st</sup> Century, Chicago.
- May A.D. (1990), *Traffic Flow Fundamentals*, Prentice Hall, Englewood Cliffs, New Jersey.
- May A.D., Roupail N., Bloomberg L., Hall, F. and Urbanik T. (2001) "Freeway Systems Research Beyond the HCM2000" Presented at the 80<sup>th</sup> Annual Meeting of the Transportation Research Board, Washington D.C. Paper No. 01-0584.

Payne H. *et al.* (1997) *Calibration of FRESIM to Achieve Desired Capacities*, Transportation Research Record, n. 1591. p. 23-30.

Van Aerde M. (1995), "Single Regime Speed-Flow-Density Relationship for Congested and Uncongested Highways," Presented at the 74<sup>th</sup> TRB Annual Conference, Washington D.C., Paper No. 95080.

Van Aerde M. and Rakha H. (1995) "Multivariate Calibration of Single Regime Speed-Flow-Density Relationships," Proceedings of the Vehicle Navigation and Information Systems (VNIS) conference, Seattle, Washington, August.

Vellendorf M. and Vortisch P. (2000), "Integrated modeling of Transport Demand, Route Choice, Traffic Flow and Traffic Emissions," Presented at the 79<sup>th</sup> TRB Annual Conference, Washington D.C., Paper No. 00459.

## APPENDIX A

The four-parameter traffic stream model that was proposed by Van Aerde (1995) and Van Aerde and Rakha (1995) is defined in Equation (A-1). The calibration of the model requires estimating the parameters  $c_1$ ,  $c_2$ , and  $c_3$ . The calculation of these parameters requires estimating four parameters, as will be demonstrated. These parameters include the free-speed ( $u_f$ ), the speed-at-capacity ( $u_c$ ), the capacity ( $q_c$ ), and the jam density ( $k_j$ ).

$$k = \frac{1}{c_1 + \frac{c_2}{u_f - u} + c_3 u} \quad [A-1]$$

Using the basic traffic stream relationship that is defined in Equation (A-2) in conjunction with Equation (A-1), the relationship between the traffic stream flow rate and speed can be derived, as demonstrated in Equation (A-3).

$$q = ku \quad [A-2]$$

$$q = \frac{u}{c_1 + \frac{c_2}{u_f - u} + c_3 u} \quad [A-3]$$

Two boundary conditions exist. The first boundary condition is that the maximum flow rate (capacity) occurs at the speed-at-capacity when the derivative of the flow rate ( $q$ ) with respect to speed ( $u$ ) is equal to zero. Consequently, by differentiating Equation (A-3) as demonstrated in Equation (A-4), Equation (A-7) is finally derived through a number of variable manipulations, as summarized in Equations (A-5) and (A-6).

$$\left. \frac{\partial q}{\partial u} \right|_{u_c} = \frac{\partial}{\partial u} \frac{u}{c_1 + \frac{c_2}{u_f - u} + c_3 u} \Bigg|_{u_c} = 0 \quad [A-4]$$

$$\frac{1}{c_1 + \frac{c_2}{u_f - u_c} + c_3 u_c} - \frac{u_c \left( c_3 + \frac{c_2}{(u_f - u_c)^2} \right)}{\left( c_1 + \frac{c_2}{u_f - u_c} + c_3 u_c \right)^2} = 0 \quad [A-5]$$

$$c_1 + \frac{c_2}{u_f - u_c} \left( 1 - \frac{u_c}{(u_f - u_c)^2} \right) = 0 \quad [A-6]$$

$$c_1 = mc_2 \quad \text{Where : } m = \frac{2u_c - u_f}{(u_f - u_c)^2} \quad [\text{A-7}]$$

The second boundary condition is that at jam density the traffic stream speed is zero. Consequently, Equation (A-8) can be derived from Equation (A-1) by setting the speed to zero at jam density. Subsequently, Equation (A-9) can be derived from Equation (A-8) through variable manipulations.

$$k_j = \frac{1}{c_1 + \frac{c_2}{u_f}} = \frac{u_f}{c_1 u_f + c_2} \quad [\text{A-8}]$$

$$c_1 = \frac{1}{k_j} - \frac{c_2}{u_f} \quad [\text{A-9}]$$

By incorporating Equation (A-9) in Equation (A-7), the headway coefficient ( $c_2$ ) can be computed using Equation (A-10) after computing the variable  $m$ . Subsequently, the headway coefficient ( $c_1$ ) can be computed using Equation (A-7).

$$c_2 = \frac{1}{k_j \left( m + \frac{1}{u_f} \right)} \quad [\text{A-10}]$$

By solving Equation (A-3) at capacity where flow equals the roadway capacity ( $q_c$ ) and the speed of the traffic stream is the speed-at-capacity ( $u_c$ ), the headway coefficient ( $c_3$ ) can be estimated using Equation (A-11).

$$c_3 = \frac{-c_1 + \frac{u_c}{q_c} - \frac{c_2}{u_f - u_c}}{u_c} \quad [\text{A-11}]$$

## LIST OF FIGURES

*Figure 1: Sample Steady-State Calibrated Car-Following Model*

*Figure 2: Comparison of Car-Following Models*

*Figure 3: Sample Traffic Stream Models (I-4, Orlando)*

*Figure 4: Sample Traffic Stream Models (Holland Tunnel, New York City)*

*Figure 5: Sample Traffic Stream Models (Arterial Road)*

*Figure 6: Comparison of Traffic Stream Models (I-4, Orlando)*

*Figure 7: Comparison of Traffic Stream Models (Holland Tunnel, New York)*

*Figure 8: Comparison of Traffic Stream Models (Arterial, UK)*

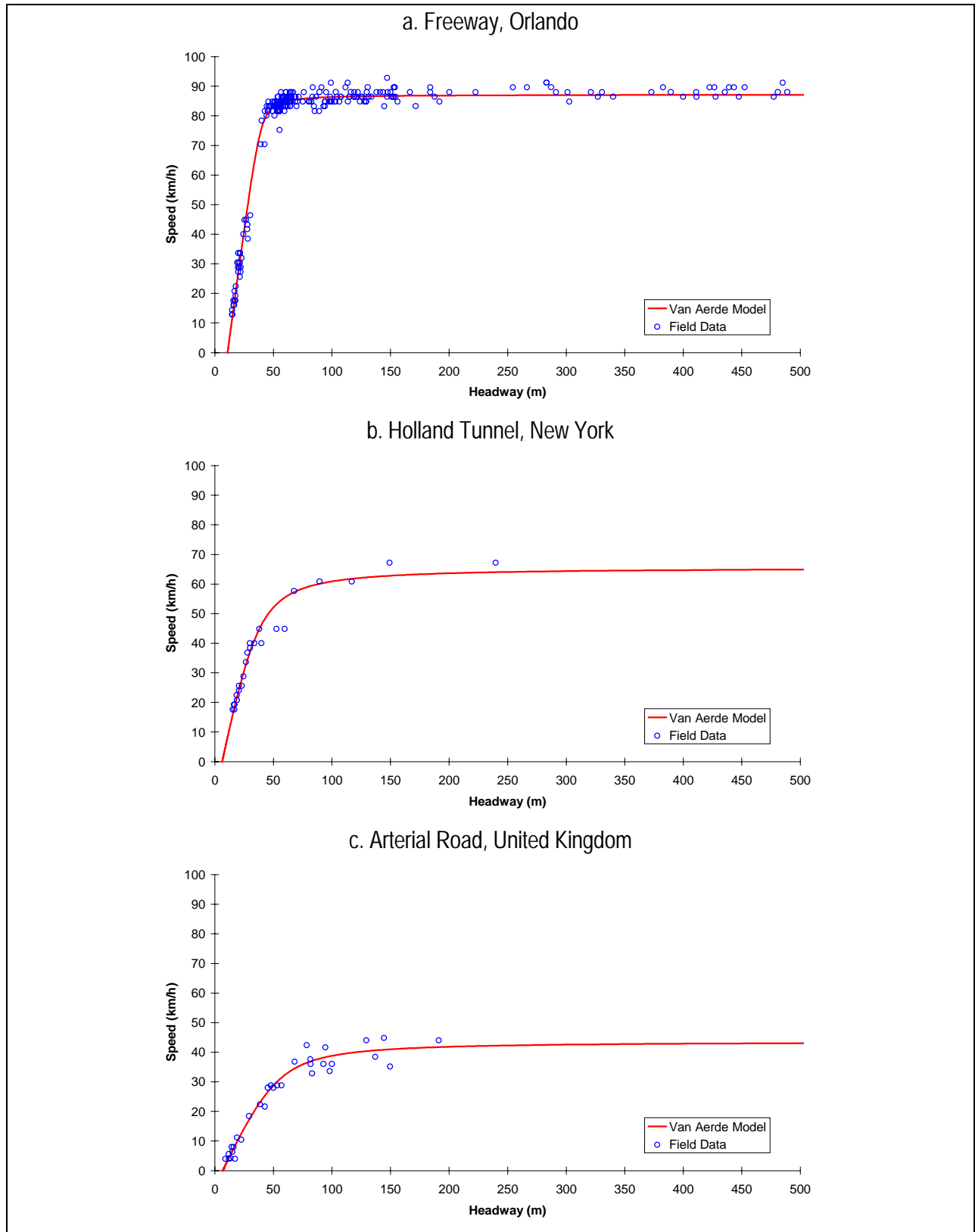


Figure 1: Sample Steady-State Calibrated Car-Following Model

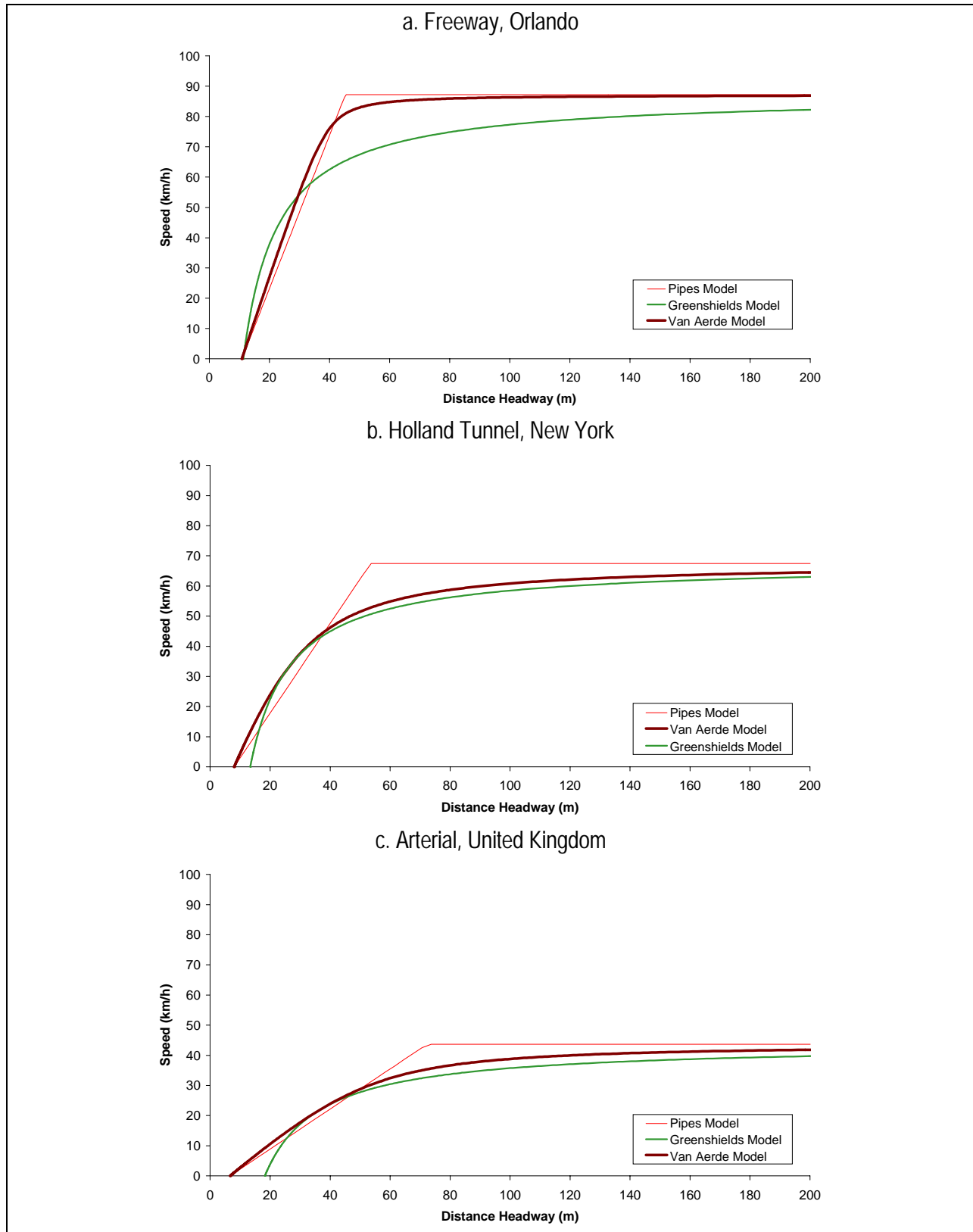


Figure 2: Comparison of Car-Following Models

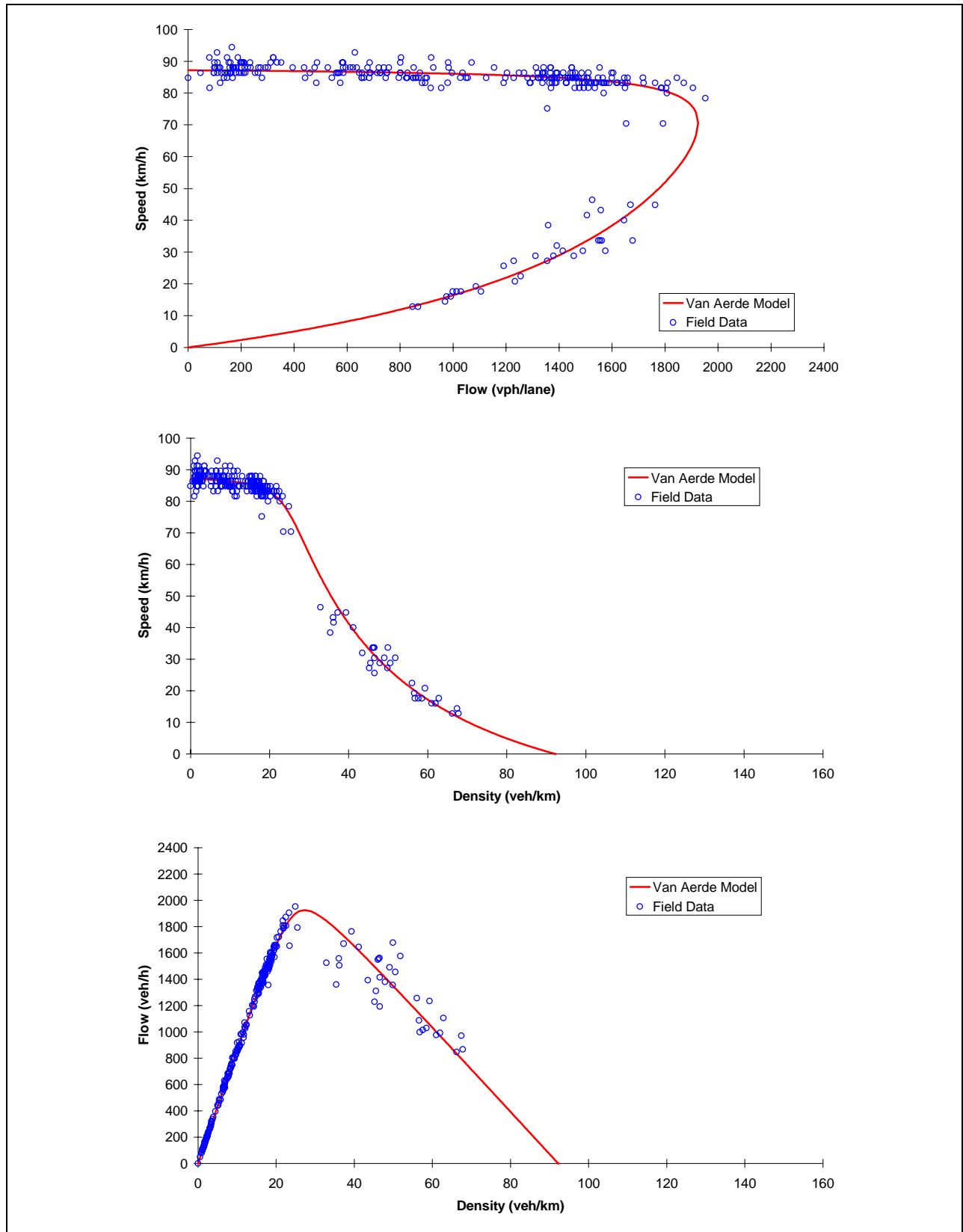


Figure 3: Sample Traffic Stream Models (I-4, Orlando)

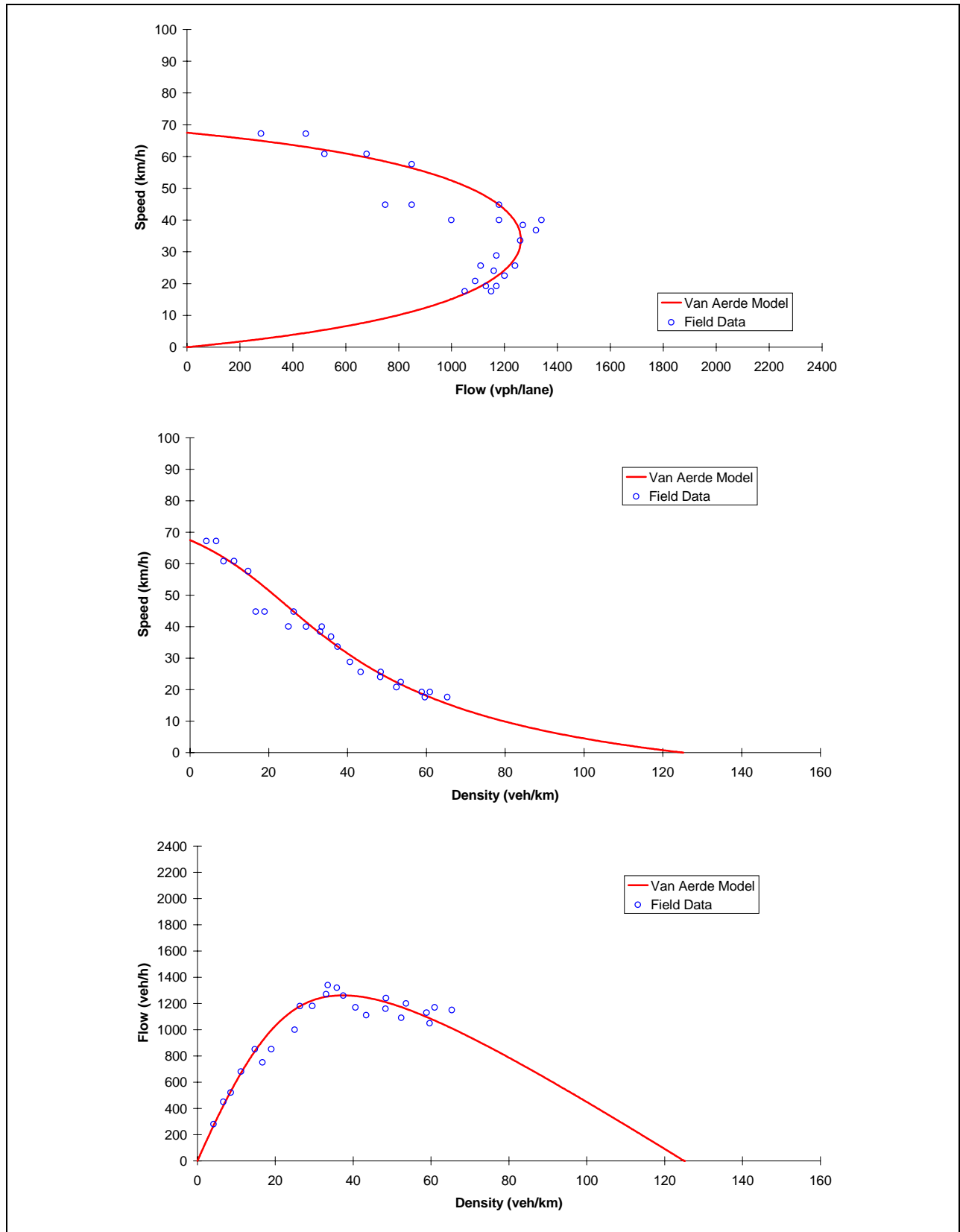


Figure 4: Sample Traffic Stream Models (Holland Tunnel, New York City)

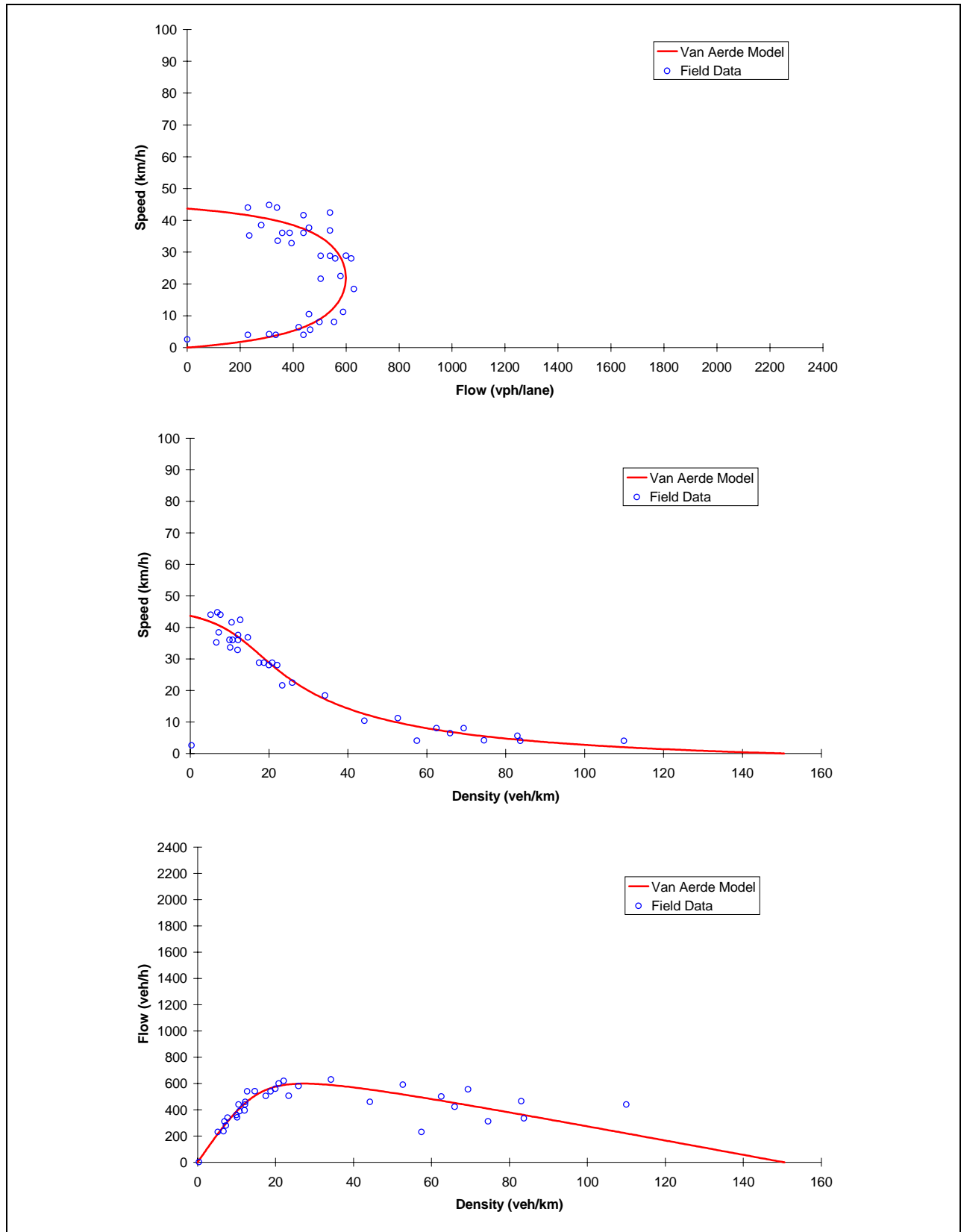


Figure 5: Sample Traffic Stream Models (Arterial Road)

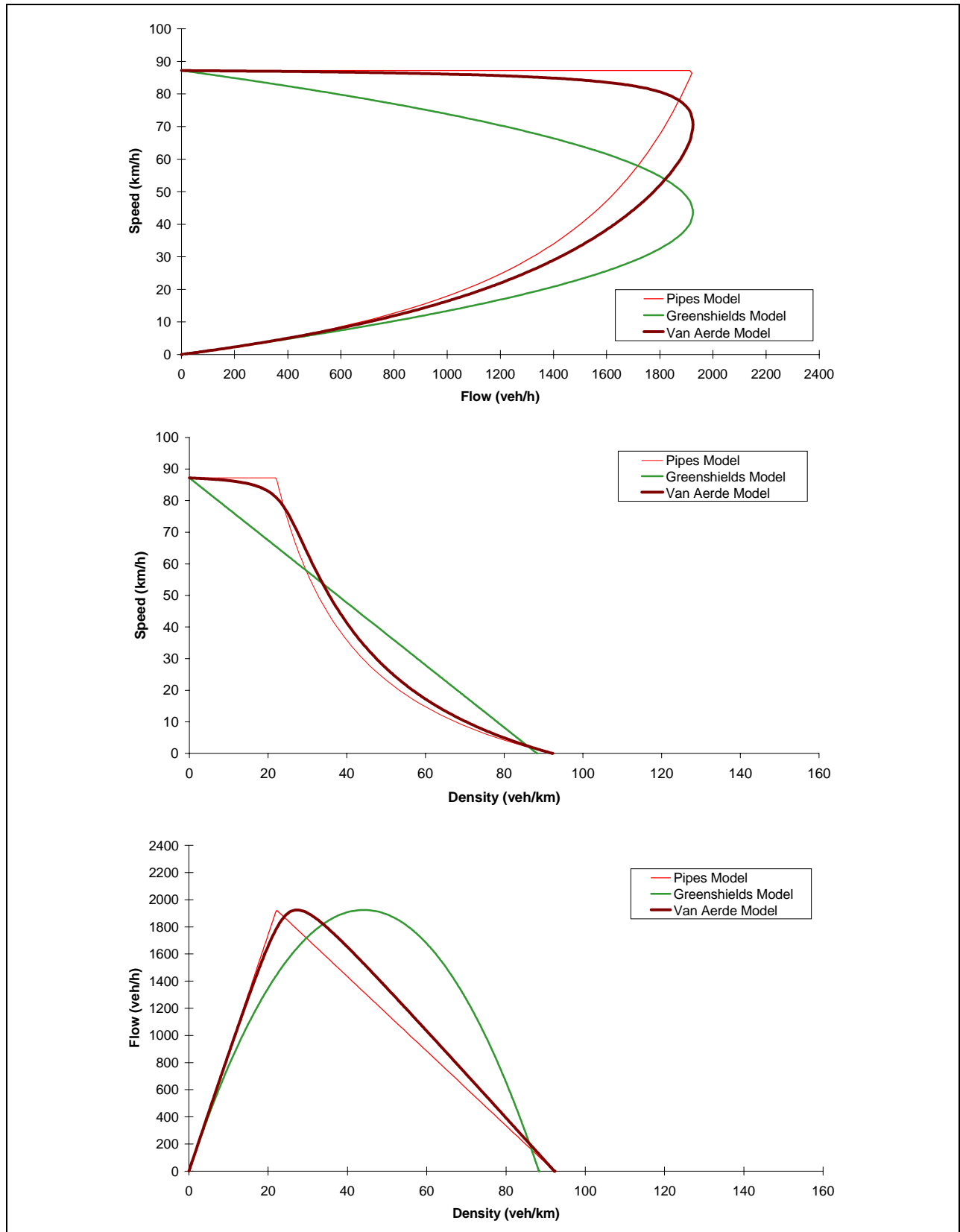


Figure 6: Comparison of Traffic Stream Models (I-4, Orlando)

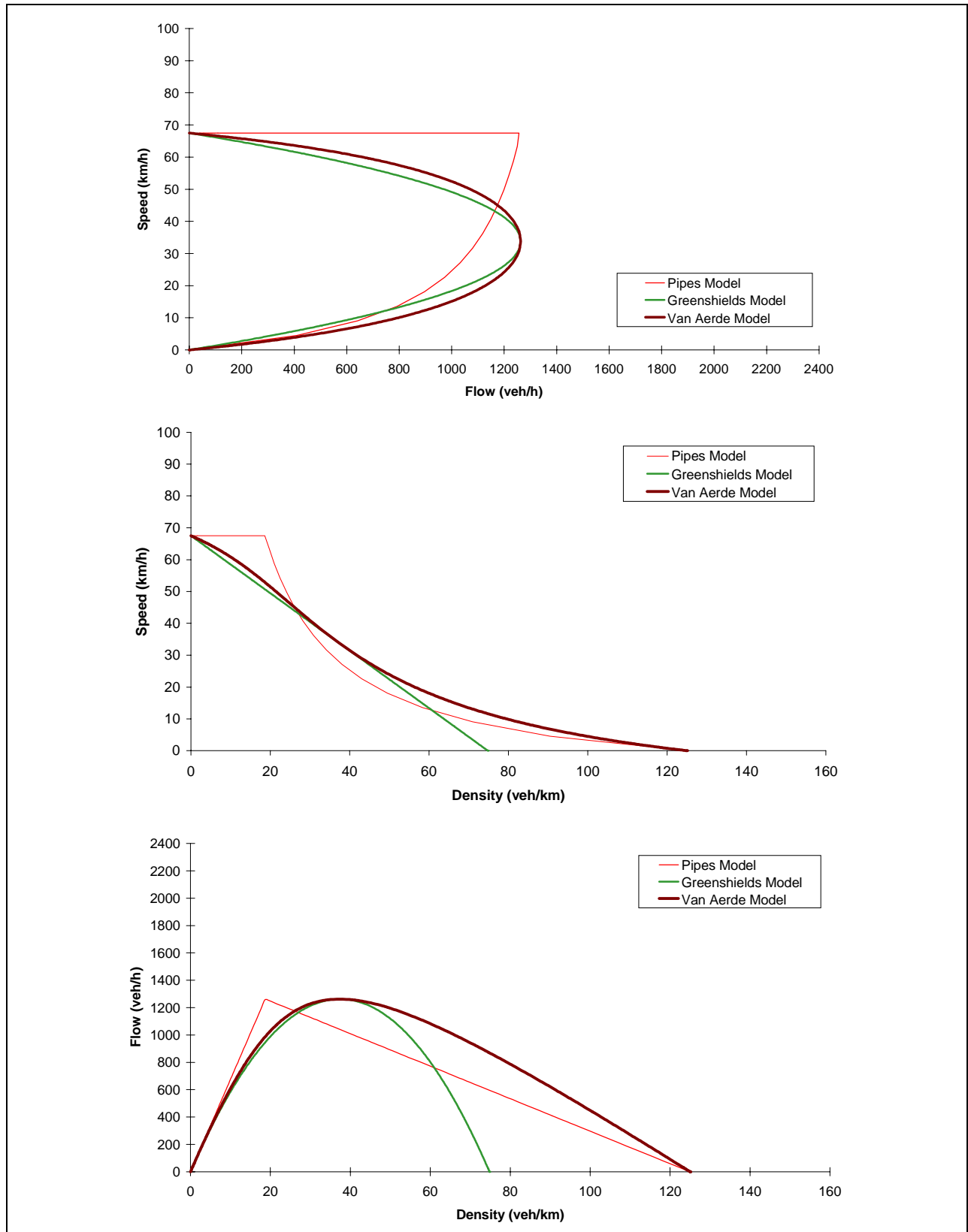


Figure 7: Comparison of Traffic Stream Models (Holland Tunnel, New York)

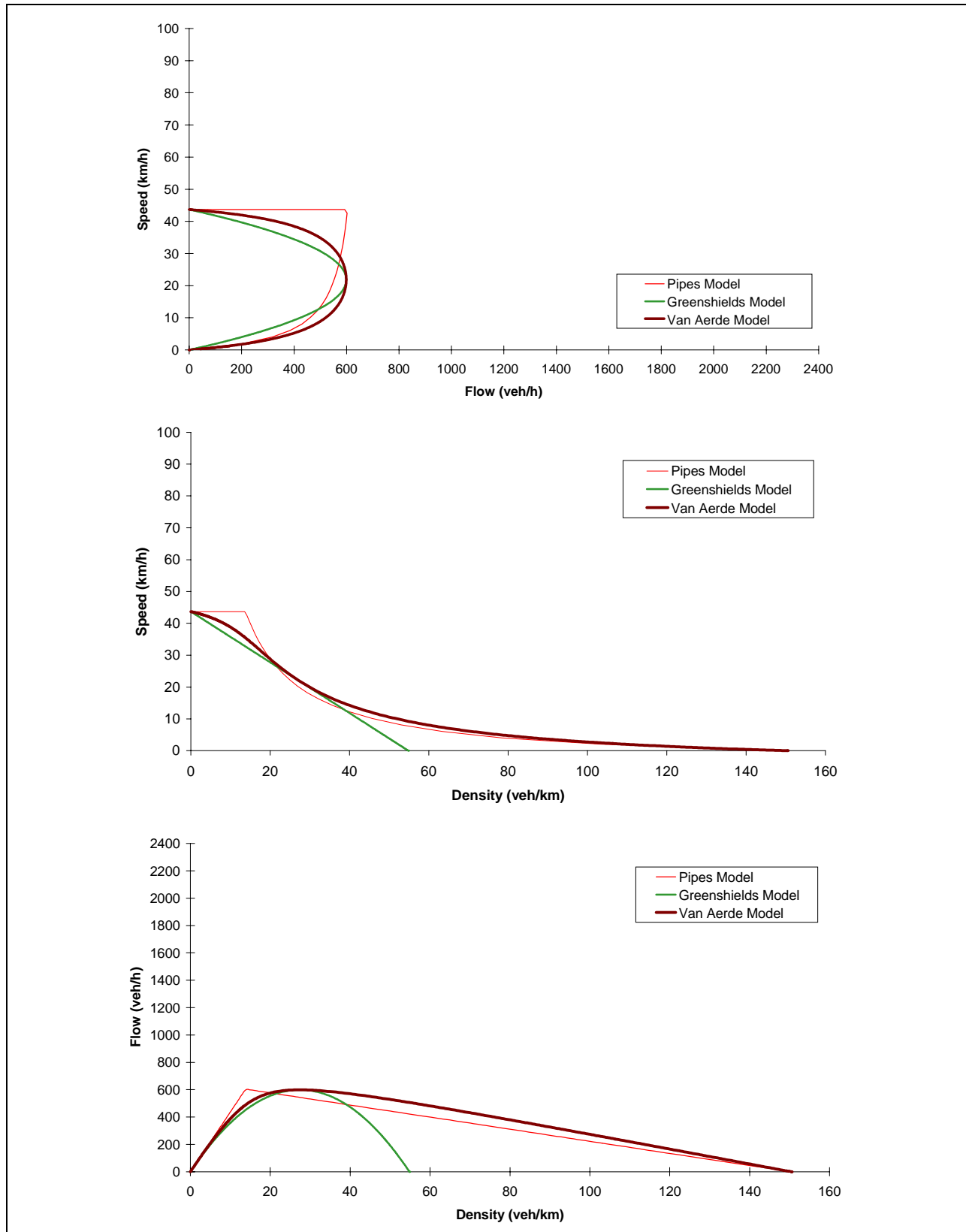


Figure 8: Comparison of Traffic Stream Models (Arterial, UK)